22nd International Conference on Renewable Energies and Power Quality (ICREPQ'24)
Bilbao (Spain), 26th to 28th June 2024
ISBN: 978-84-09-60656-6

Enhancing Wind Turbine and Fuel Cell Voltage Stability with Distribution Static Compensator

Ahmed S. Menesy[1], I. A. Saeed[1], Waleed M. Hamanah[1,2,*], Hamed M. Sultan[3], Luai Alhems[2,4], and M. Abido[1,5,6]

[1] Electrical Engineering Department, College of Engineering and Physics, KFUPM, Dhahran 31261, Saudi Arabia
[2] Applied Research Center for Metrology, Standards and Testing, Research & Innovation, KFUPM Dhahran, 31261, Saudi Arabia
[3] Electrical Engineering Department, Faculty of Engineering, Minia University, Minia 61517, Egypt
[4] Applied Research Center for Environment and Marine Studies, Research & Innovation, KFUPM, Dhahran 31261, Saudi Arabia
[5] IRC for Sustainable Energy Systems, Research & Innovation, KFUPM Dhahran, 31261, Saudi Arabia
[6] SDAIA-KFUPM Joint Research Center for Artificial Intelligence, KFUPM, Dhahran 31261, Saudi Arabia

Corresponding author: Waleed M. Hamanah

Abstract- Integrated wind farms face significant challenges due to strict grid code requirements. Maintaining voltage stability is especially important for wind farms that are connected to the electrical grid. This research paper examines how FACTS devices, specifically Static Synchronous Compensators (STATCOMs), can be used to resolve voltage stability issues in wind farms and fuel cell power plants that employ Double Fed Induction Generators (DFIGs) and are connected to both loads and the power grid. During fault ride-throughs and power outages, wind farms face challenges such as voltage dips and fluctuations, which can negatively impact the grid. As a result, wind turbines require a stable grid to function effectively. In the absence of voltage stability measures, wind farms may experience reduced productivity, equipment failure, and downtime. As a dynamic voltage restorer, FACTS devices will be used. Thus, stable voltage levels are maintained, and power interruptions are prevented at DFIG-based wind farms. Three-phase impedance faults on load buses and 25% voltage sags on high voltage buses were examined in this study. STATCOMs were implemented as dynamic voltage restorers during fault ride-throughs and power grid disruptions in the MATLAB/SIMULINK simulations to mitigate voltage dips and fluctuations experienced by wind farms and fuel cells. Simulation results showed that STATCOMs significantly reduced downtime, increased power output, and minimized equipment failures in wind farms.

Index terms: *DFIG, Wind turbine, short circuit, Voltage Sag and STATCOM.*

I. Introduction

As renewable energy technologies have become more prevalent in electrical grids, engineers and researchers are placing more emphasis on optimizing the conversion of wind energy to electrical energy and ensuring the stable performance of wind farms that are connected to the power grid. This has resulted in the emergence of innovative technologies for systems that convert wind energy into electricity. At present, the most commonly used technology is the DFIG based variable speed wind energy conversion system, which offers numerous advantages [1]-[5]. The DFIG system involves linking the induction generator to the power grid via connecting both the stator and rotor terminals using a partially rated AC/DC/AC converter that operates at variable frequencies. Although using wind power as a source of clean and renewable energy has many benefits, introducing a large amount of wind power into the electrical system can also give rise to fresh problems and challenges that require attention. To tackle these issues, a combination of wind power generation and hydrogen-based power generation could greatly enhance the supply security of the power grid, leading to improved operational efficiency for the utilities that maintain it [6]-[9].

When a wind turbine (WT) that utilizes a DFIG is linked to an electric grid that has a low short circuit ratio and is considered weak., in the event of a grid disturbance or heavy load operation, the WT may not be capable of providing adequate reactive power and voltage support. because the grid-side converter (GSC) has limited power capacity [10]-[12]. This situation may result in instability of the voltage, the possibility of the WT being disconnected from the grid, and damage to the DFIG's power electronic converters due to high induced voltage. So, transient voltage stability is a crucial aspect of power system operation. It pertains to the capacity of the power system to keep the voltage level within acceptable parameters during regular and irregular circumstances. Voltage stability is affected by various factors such as load demand, generation capacity, and transmission system constraints. Voltage instability can lead to voltage collapse and blackout, which can have severe consequences on the power system and the connected loads. In recent years, the integration of renewable energy sources (RES) such as photovoltaic (PV) systems and solid oxide fuel cell (SOFC) has gained significant attention due to their environmental and economic benefits. However, the integration of RES has a great effect on the voltage stability of the electrical grid, especially in a distribution network. The integration of renewable energy systems into the power grid can lead to voltage instability due to their variable nature. To mitigate this problem, researchers have proposed various solutions, including the use of Distribution Static Compensator (DSTATCOM) to enhance the transient voltage stability of PV/fuel cell systems [9], [13], [14].

There are various techniques that have been developed for voltage stability enhancement, such as [15]-[19]. ***FACTS Devices*** are power electronics-based devices that can provide voltage control and enhance the power system voltage stability.

The most commonly used FACTS devices for voltage stability enhancement are Static Var Compensator (SVC), STATCOM, and Unified Power Flow Controller (UPFC). These tools introduce reactive power into the power system to reinforce voltage and ensure its stability. ***Control Methods***, various control methods have been proposed for voltage stability enhancement. Some of the commonly used control methods are proportional-integral-derivative (PID) control, fuzzy logic control, and adaptive control. These control methods are used to regulate the output of FACTS components and maintain the system voltage stability. ***Renewable Energy Sources***, the incorporation of RES, like wind and solar power, into the power grid has a noticeable effect on voltage stability. The intermittent nature of these sources can cause voltage fluctuations and instability. However, through the utilization of energy storage systems and sophisticated control methods, it is possible to preserve the voltage stability of the power system. ***Load Shedding***, load shedding is a method employed in emergency situations to ensure the stability of the power system. In case of voltage instability, load shedding can be used to reduce the demand on the system and maintain the system voltage stability. ***Power System Planning***, power system planning is an essential aspect of voltage stability enhancement. Determining the most effective location for FACTS components, transmission lines, and generators can improve the voltage stability of the system. Furthermore, proper planning can help in reducing the power losses and improving the overall efficiency of the system.

To ensure that WTs equipped with DFIGs operate without interruptions, it is essential to maintain voltage stability. When connected to the grid, DFIGs FIGs) can produce both active power and reactive power autonomously. However, because of their limited reactive power capacity and remote location, they are unable to supply enough reactive power support without an external dynamic reactive power compensation device. Shunt FACTS devices such as SVC, Unified Power Flow Controllers (UPFC), and STATCOM Have been extensively employed to attain superior steady-state and transient control of voltage [10], [20].

This research aims to investigate the voltage stability of a medium-power wind park (9MW) that is linked to a distribution grid and has a hydrogen-based storage system. To achieve this goal, the entire system will be modeled, including the wind farm with DFIG, SOFC-based energy storage system, a DC/DC converter with a boost function and a three-phase inverter that features active and reactive power control. The primary goal of this research can be summarized as:

- Modeling for a wind energy conversion system that operates at variable speeds and utilizes a DFIG as a power generation unit.
- Modeling, control, and operation of a SOFC Power Plant in grid connected system.
- Modeling the microgrid system (WT/FC) integrated with the grid.
- Examining how grid faults impact the dynamic performance of a variable-speed wind-driven DFIG when linked to the grid.
- Studying the impact of STATCOM on enhancement of transient voltage stability of proposed hybrid system.

II. MODELING OF POWER SYSTEM COMPONENTS

This section will cover the creation of models for various power system components, including DFIG wind turbines, SOFCs, and STATCOMs.

A. Modeling of Wind Power Plant

The composition of modern wind power plants involves various components, including the rotor, gearbox, DFIG. The following sections provide an explanation of the WT and DFIG modeling. The power-speed parameters of WT are crucial in determining its aerodynamic behavior. Both the wind speed and the rotor speed have an impact on how much power the turbine produces. The following equation can be used to mathematically express the power that the turbine is able to capture [21].

$$P_m = \frac{1}{2}\rho A U^3 c_p(\beta, \lambda) \quad (1)$$

In the given equation, the variables represent the following: ρ denotes air density in (kg/m³), A represents the cross-sectional area of the WT rotor in (m²), U signifies the wind speed in (m/s), and Cp (β, λ) represents the power coefficient, which is dependent on both the pitch angle β and tip speed ratio (λ). λ is formulated as follows [22]:

$$\lambda = \frac{\omega_T R_T}{U} \quad (2)$$

In the equation provided, ω_T denotes the angular speed of WT rotor, and RT represents the radius of WT rotor in meters (m). Figure 1 displays the power coefficient function Cp as a function of λ, and it is parameterized with respect to the pitch angle β. Based on Figure 1, it is clear that to achieve maximum energy capture, at all wind speeds, it's essential to maintain the ideal tip speed ratio, which equates to the greatest power coefficient. DFIG, both in its stationary and rotating components, is equipped with windings that efficiently transmit a significant amount of power from the shaft to the electrical system. These doubly fed machines are commonly utilized in applications where a constant power system frequency is desired alongside variable machine shaft speed.

Figure 2 provides an illustration of the WT and DFIG. The AC/DC/AC converter is composed of two primary subsystems: The first one is the Rotor-Side Converter (RSC) that takes this name because it is connected to the rotor and the Grid-Side Converter (GSC) that is connected directly to the grid. These converters utilize Insulated Gate Bipolar Transistors (IGBTs) in order to transform DC voltage into AC voltage. A capacitor on the DC side is linked to the DC voltage source. The Park equations can be used to model the dynamics of the doubly fed induction generator [10]. Based on this principle the voltages appeared on the stator and rotor terminals are written as follows [22]:

$$V_{qs} = R_s I_{qs} + \frac{d\psi_{qs}}{dt} + \omega_e \psi_{ds} \quad (3)$$

$$V_{ds} = R_s I_{ds} + \frac{d\psi_{ds}}{dt} - \omega_e \psi_{qs} \quad (4)$$

$$V_{qr} = R_r I_{qr} + \frac{d\psi_{qr}}{dt} + (\omega_e - \omega_r)\psi_{dr} \quad (5)$$

$$V_{dr} = R_r I_{dr} + \frac{d\psi_{dr}}{dt} - (\omega_e - \omega_r)\psi_{qr} \quad (6)$$

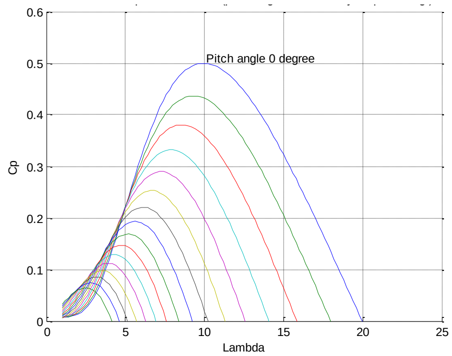

Figure 1: Cp as function of λ.

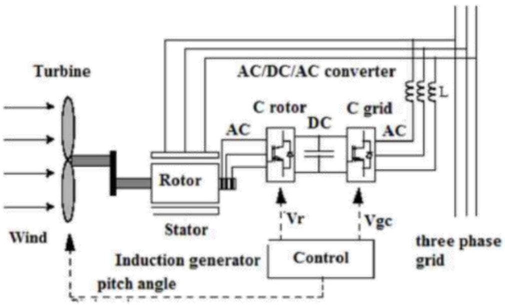

Figure 2: DFIG structure.

The electromagnetic torque generated by the DFIG can be represented as a function of the torque provided by the turbine.

$$T_e = \frac{3}{2}\frac{P}{2}\left(\psi_{ds} I_{qs} - \psi_{qs} I_{ds}\right) = 2H\frac{d\omega_m}{dt} + \omega_m T_m \quad (7)$$

In the given context, the variable T_m represents the mechanical output torque. The active and reactive power generated in the stator can be computed using the following equations:

$$P_s = \frac{3}{2}\left(V_{ds} I_{ds} + V_{qs} I_{qs}\right) \quad (8)$$

$$Q_s = \frac{3}{2}\left(V_{qs} I_{ds} - V_{ds} I_{qs}\right) \quad (9)$$

To regulate the WT generation, the DC bus voltage and either the reactive power or the grid terminal voltage, the control system generates voltage commands (Vr and Vgc) and a pitch angle command for the RSC and GSC, correspondingly.

B. Modeling of SOFCs Stack

The fundamental physical construction of an FC comprises a porous anode and cathode on opposite sides of an electrolyte layer that are in direct contact with each other. A schematic diagram in Figure 3 illustrates a fuel cell, indicating the flow directions of reactant and product gases as well as ion conduction. In a conventional fuel cell, an electrochemical reaction occurs at the electrodes, resulting in the generation of an electric current. An oxidant, such as oxygen, is continually delivered to the anode, while gaseous fuels are continually provided to the cathode. The electrolyte of SOFCs is made of solid, nonporous metal oxide ZrO_2 that has been stabilized with Y_2O_3 [20]-[23]. Energy gets released in this reaction. At the cathode, the combination of oxygen with H+ ions and electrons absorbed from the electrode results in the production of water.

$$E = N_0\left(E_0 + \frac{RT}{2F}\left[\ln\frac{p_{H2}\, p_{O2}^{0.5}}{p_{H2O}}\right]\right) \quad (10)$$

E indicates both the partial pressures of reactants and byproducts in a system as well as the ideal equilibrium potential, which changes with temperature, while E_0 represents the ideal standard potential of individual FC. The series connected cells connected is denoted by No, the gas constant is denoted by R (8.31 J/mol·K), the working temperature of the SOFC is denoted by T, the Faraday constant is denoted by F (96487 C/mol), while the partial pressures of H2, O2, and H2O are denoted by P_{H2}, P_{O2}, and P_{H2O}, respectively.

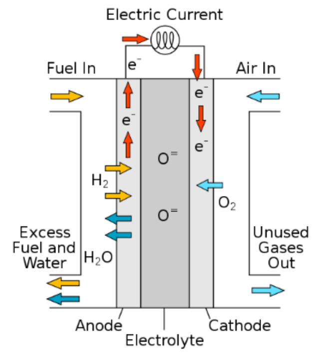

Figure 3: Diagram of a single SOFC.

The generated voltage of the FC stack can be changed to the necessary dc bus voltage using a boost dc/dc conver that is controlled by a traditional PI controller. The required (860 V) on the DC voltage bus is compared to the converter output voltage, while PI controller receives the error signal in order to operate the PWM pulse generator. To regulate the power electronic switch, the PWM pulse generator is going to produce pulse sequences with the desired duty ratio. Controlled switching is implemented to regulate the output voltage within a predetermined range in this study. Specifically, the output voltage is kept within a range of 0.58% (from 855 to 865 V) through the application of controlled switching techniques.

The output of the Voltage Source Inverter (VSI) must be shaped and managed in order to satisfy the prerequisites for connecting the SOFC stack to a grid and efficiently manage the flow of active and reactive components of power [24]. For the inverter, a sinusoidal PWM (SPWM) controller is created to manage reactive and actual power as well as satisfy voltage regulation. A control system that uses an inner current control loop and an exterior voltage regulator to regulate both real and reactive power. The inverter was controlled in this study using this control method. The control system employs the abc/dq0 transformation method to convert time-varying variables from a fixed abc frame of reference to DC signals within a rotating d_{q0} frame of reference that is synchronized with the system's dynamics. This transformation simplifies the control algorithms and enhances the system's control efficiency. It enables accurate regulation of the system's behavior in the d_{q0} frame, leading to improved control performance and operational effectiveness. Next, the voltage and current controllers receive the d_{q0} signals as inputs. The voltage and current controllers are selected as PI compensators.

C. *Modeling of STATCOM*

The STATCOM capacitive is supporting the system's voltage during low system voltage conditions. In contrast, the STATCOM draws inductive power (STATCOM inductive) when the grid voltage is high in order to control and stabilize the voltage. A voltage source converter (VSC) that is coupled to the secondary winding of the transformer couple, regulates the amount of reactive power. The VSC transforms the constant DC voltage into the necessary value represented by V2 by using power electronic components like Gate Turn-Off thyristors (GTOs), Insulated Gate Bipolar Transistors (IGBTs), or Integrated Gate-Commutated Thyristors (IGCTs). The interchange of active and reactive power between the two voltage sources, V_1 (voltage source) and V_2, which is produced by the VSC [14] as an illustration of the STATCOM's working principle. The STATCOM has the ability to control and maintain the system voltage thanks to this exchange.

Figure 4 shows the STATCOM's control system, which includes a phase-locked loop (PLL) that synchronizes with the three-phase primary voltage's positive sequence component, V1. The direct-axis (Vd) and quadrature-axis (Vq) components of the AC voltages, as well as the direct-axis (Id) and quadrature-axis (Iq) components of the AC currents, are calculated using the PLL's output. These variables are essential to the management and operation of STATCOM. Measurement systems are utilized to measure the DC voltage V_{dc}, and the d and q components of the AC voltages and currents that necessitate control and management.

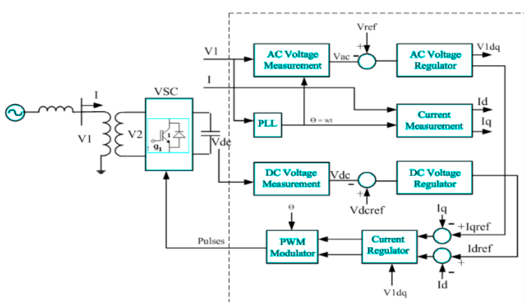

Figure 4: Schematic Diagram of STATCOM control system.

AC and DC voltage regulators make up the STATCOM's external regulation loop. While the DC voltage regulator creates the base current (I_{dref}) for the current regulator, the AC voltage regulator generates the base current (I_{qref}). The PWM converter (V_{2d}, V_{2q}) controls the current regulator, which is a component of the inner current regulation loop and is in charge of controlling the amplitude and phase of I_{dref} and $_{Iqref}$. A feed-forward type regulator uses V_1 measurements (V_{1d}, V_{1q}) and the transformer's leakage reactance to forecast the V2 voltage output (V_{2d}, V_{2q}), improving the current regulator's performance. Power flow between the AC system and the STATCOM is effectively managed by altering the magnitude and phase of the STATCOM's produced voltage. The reference currents are represented by the controller outputs Id_ref and Iq_ref in dq coordinates. Equations (11) and (12) show how important these reference currents are for estimating the power supplied by the STATCOM [9].

$$P_{inj} = V_i\left(I_d \cos\theta_i + I_q \sin\theta_i\right) = V_d I_d + V_q I_q \quad (11)$$

$$Q_{inj} = V_i\left(I_d \sin\theta_i - I_q \cos\theta_i\right) = -V_d I_q + V_q I_q \quad (12)$$

Through the manipulation of these control variables, the STATCOM can efficiently handle and oversee the reactive power and current flow, ensuring the maintenance of the desired system performance and stability.

III. SIMULATION RESULTS AND DISCUSSIONS

Simulations were run using MATLAB SIMULINK to assess the impact of the STATCOM on the voltage profile of a weak grid [25]. The study aimed to assess the performance of the grid under various transient scenarios, including a three-phase fault, sudden load shift, and voltage sag on the high voltage bus of the system. The system comprises six Doubly Fed Induction Generators. These DFIGs operate under similar conditions. The external grid utility to which the proposed wind farm and SOFC systems are integrated has a limited short circuit capacity of 50 MVA, indicating its weakness in responding to disturbances in the system. Additionally, a 5 MW load is integrated into the entire system via the load bus. The voltage at the load bus is stepped down to 600V. The DFIG Wind Turbines run at a power factor that is nearly unity, resulting in negligible reactive power generation. The active power required by the load is divided between the DFIG and the SOFC. According to the previous analysis, a 1.25 kV/30 kV transformer connects a STATCOM, which acts as an active component for voltage support, to the system.

- *Case one: Three-Phase to Ground Fault*

The impact of a three-phase short circuit fault with high impedance (X_f=3) subjected to the terminals of the load is analyzed. The fault begins at t=2.0 seconds and lasts until t=2.2 seconds. Two scenarios are considered in this case: (i) without any compensation, and (ii) with a 20 MVA rated STATCOM. The voltage measured at the terminals of the load (referred to as the fault bus) is depicted in Figure 5 for both test cases. Without a compensating device, after the defect has been fixed, the voltage takes a while to recover. Utilizing STATCOM will help with reactive power, faster recovery times, and the use of constant voltage. The voltage at the DFIG bus is depicted in Figure 6 for the two scenarios. Due to the system's need for some reactive power to assist in stabilizing the voltages at various nodes, this voltage's recovery time is more than that in the case of load voltage. When STATCOM is used, the time required is less than it would be if no compensating devices were used. The voltage at the SOFC bus is depicted in Figure 7. Due to STATCOM's sole responsibility for meeting the system's overall reactive power demand, the SOFC continues to function correctly even when there is a failure. During a fault, STATCOM's reactive power assistance helped to raise voltage magnitude at all power system buses. The voltage signals measured at the common bus are presented in Figure 8. By integrating a STATCOM into the system, numerous advantages can be observed when a fault occurs. Firstly, during the fault, the presence of a STATCOM results in an elevation of the bus voltage, offering support to the system's voltage. This assists in reducing the adverse impacts of the fault and maintaining stable voltage levels. Moreover, the utilization of a STATCOM facilitates a faster recovery time after the fault is cleared. It accomplishes this by injecting reactive components into the grid and effectively managing the voltage levels. Consequently, STATCOM aids in swiftly restoring the system to its normal operating condition. This leads to minimized downtime and enhanced overall stability and performance of the power system.

Figure 9 illustrates the active and reactive powers supplied by the STATCOM, while Figure 10 displays its terminal voltage on both the ac and dc sides. At t = 2.0 sec, a three-phase fault at the terminals of the load is simulated. The fault is formulated through high impedance. Consequently, this causes a drop in voltage at the fault bus. This triggers the behavior of the STATCOM. The magnitude of the required reactive power depends on how much voltage is dropped. Even in low voltage environments, the device is intended to function well. In these circumstances, the STATCOM supplies its allotted reactive power to guarantee voltage stability at the faulted bus.

At t=2.2 sec, time of fault clearance, until t=2.3 sec, when the system has fully recovered, the STATCOM assists the RSC in returning to full functionality. As the fault is fixed at t=2.2 seconds, the voltage starts to rise, and the reactive power generated from the device exceeds the required amount. However, since this overshoot remains well within the carrying capacity and limits of the STATCOM, it can be disregarded as a transient. At t=2.0 and t=2.2 sec, an insignificant value of real power exchange takes place, accompanied by a transient recorded in the dc voltage of the STATCOM.

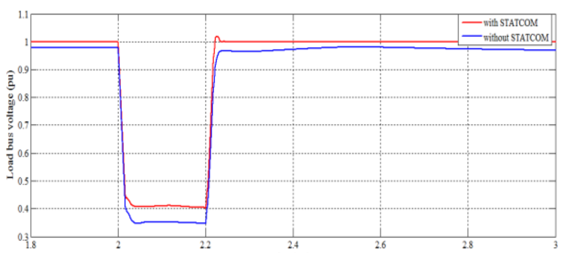

Figure 5: Load bus voltage under three phase faults.

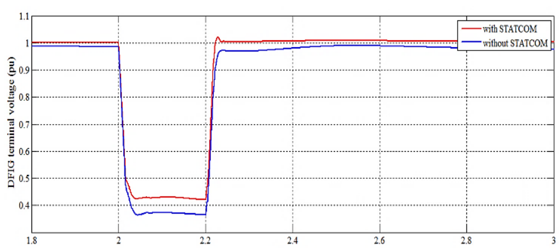

Figure 6: DFIG bus voltage under three phase faults.

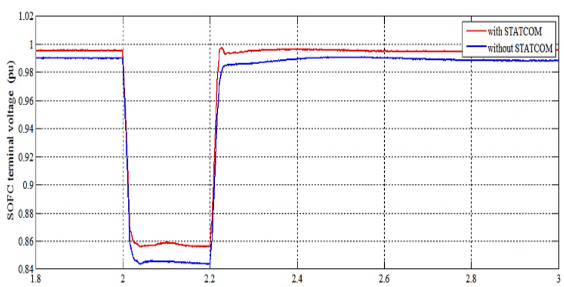

Figure 7: SOFC bus voltage under three phases faults.

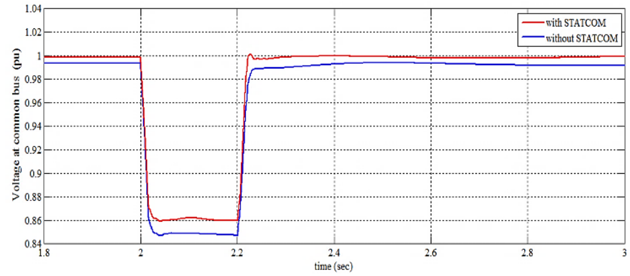

Figure 8: Voltage at the common busbar under three phase faults.

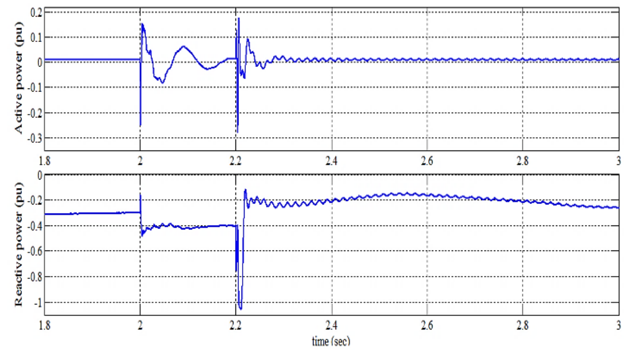

Figure 9: STATCOM generated power under three phase faults.

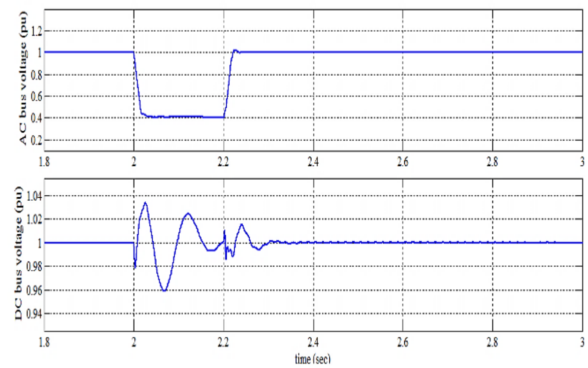

Figure 10: AC and DC bus voltages under three phase faults.

➢ *Case two: 25% Voltage Sag at the Infinite Bus*

At t=2.0 seconds, there was a voltage sag of 25% of the rated voltage at the 25kV bus, and the problem was resolved at t=2.2 seconds. Figure 11 illustrates the voltages measured at the AC and DC bus, and its behavior mirrors that of the three-phase fault case. The DC bus voltage experiences a step disturbance at the occurrence of the fault (t=2.0 sec) and its clearance (t=2.2 sec). However, the control system effectively maintains a constant voltage throughout the entire duration, ensuring stability and reliable operation of the STATCOM.

Figure 12 displays information about the reactive and active power components of the STATCOM. Throughout the fault period, the STATCOM possesses a vital function in enhancing the voltage across all nodes by injecting reactive power into the system. This helps in the stabilization and support of voltage levels. The real power generation of the STATCOM is subject to changes due to variations in the DC bus voltage during the fault occurrence and clearance. The fluctuations in the DC bus voltage impact the real power produced from the STATCOM during these fault events.

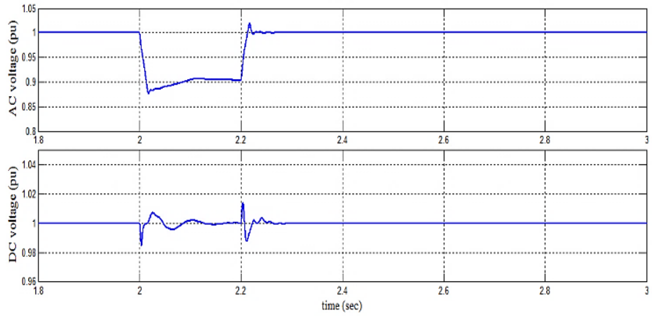

Figure 11: AC and DC bus voltages of the STATCOM for 25% voltage sag.

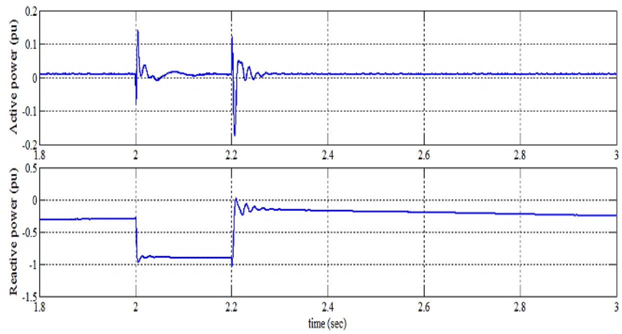

Figure 12: Active and Reactive power of the STATCOM for 25% voltage sag.

IV. Conclusion

This research focuses on the integration of a wind farm with the utility grid, incorporating SOFC. A dynamic model has been developed and presented to analyze this integration process. To prevent excessive charging of auxiliary storage devices and ensure a rapid response from the fuel cell, a novel technique has been proposed. This technique involves making simultaneous step and ramp changes in the fuel cell reference power. Remarkably, the fuel cell exhibited a response rate that exceeded expectations. The study also explores the implementation of a three-phase VSI model with a PQ control approach, which demonstrates a fast and accurate response. As a result of this control approach, the integrated DFIG Wind Park + SOFC system is now capable of generating reactive power. In particular, the research focuses on modeling a DFIG within the system. The DFIG requires adjustments in reactive power during disturbances on the grid side. To address this, a properly sized STATCOM can be employed to correct the reactive power when connected to an unstable grid. According to simulation tests, the STATCOM's additional voltage and reactive power support considerably improves the turbine ability to recover from faults by hastening the restoration of voltage characteristics.

Acknowledgment

The author would like to acknowledge the support provided by the Applied Research Center for Metrology, Standards and Testing (ARC-MST) and the Deanship of Research Oversight and Coordination (DROC), through Grant No. INRE2330, Research and Innovation, King Fahd University of Petroleum &and Minerals (KFUPM)

REFRENCES

[1] S.-B. Lee, K.-B. Lee, D.-C. Lee, and J.-M. Kim, "An improved control method for a DFIG in a wind turbine under an unbalanced grid voltage condition," *Journal of Electrical Engineering and Technology*, vol. 5, no. 4, pp. 614-622, 2010.

[2] S. Yousefikhah, E. Asgharizadeh, and M. Jahangir, "Multi-objective optimization of a hybrid micro-grid system for reducing grid dependency in the automotive industry: a case study of Iran Khodro company," *International Journal of Modelling and Simulation*, pp. 1-23, 2023.

[3] R. Narayana Sarma, V. Kumar, S. Lal SR, M. Reghunath, A. Jayan, and A. Suryan, "Wind power resource assessment and wind-hydrogen generation potential: a case study," *Energy Sources, Part A: Recovery, Utilization, and Environmental Effects*, pp. 1-17, 2022.

[4] O. Tang, J. Rehme, and P. Cerin, "Levelized cost of hydrogen for refueling stations with solar PV and wind in Sweden: On-grid or off-grid?," *Energy*, vol. 241, p. 122906, 2022.

[5] O. M. Kamel, A. A. Z. Diab, M. M. Mahmoud, A. S. Al-Sumaiti, and H. M. Sultan, "Performance enhancement of an Islanded microgrid with the support of electrical vehicle and STATCOM systems," *Energies*, vol. 16, no. 4, p. 1577, 2023.

[6] N. J. Schenk, H. C. Moll, J. Potting, and R. M. Benders, "Wind energy, electricity, and hydrogen in the Netherlands," *Energy*, vol. 32, no. 10, pp. 1960-1971, 2007.

[7] W. M. Hamanah, "A Lightning Search Algorithm for Optimal Planning of Power Systems With Short/Long-Term Storage," in *IEEE Access*, vol. 12, pp. 16682-16695, 2024, doi: 10.1109/ACCESS.2024.3356726.

[8] P. Rani and S. Kumar, "Probabilistic Analysis of Wind Integrated Power System Considering 3-phase Line Fault," in *2022 IEEE 10th Power India International Conference (PIICON)*, 2022, pp. 1-6: IEEE.

[9] I. Etxeberria-Otadui, U. Viscarret, I. Zamakona, B. A. Redondo, and J. Ibiricu, "Improved STATCOM operation under transient disturbances for wind power applications," in *2007 European Conference on Power Electronics and Applications*, 2007, pp. 1-10: IEEE.

[10] M. Sheikh, S. Muyeen, R. Takahashi, and J. Tamura, "Smoothing control of wind generator output fluctuations by PWM voltage source converter and chopper controlled SMES," *European Transactions on Electrical Power*, vol. 21, no. 1, pp. 680-697, 2011.

[11] P. Barra, W. de Carvalho, T. Menezes, R. Fernandes, and D. Coury, "A review on wind power smoothing using high-power energy storage systems," *Renewable and Sustainable Energy Reviews*, vol. 137, p. 110455, 2021.

[12] A. Božiček, B. Blažič, and I. Papič, "Time–optimal current control with constant switching frequency for STATCOM," *Electric Power Systems Research*, vol. 80, no. 8, pp. 925-934, 2010.

[13] G. S. S. Goad, "Mitigation of Reactive Power Control of Renewable Wind Energy Source Using Reactive Power Control Device," *Journal homepage: www. ijrpr. com ISSN*, vol. 2582, p. 7421.

[14] A. P. Jayam and B. H. Chowdhury, "Improving the dynamic performance of wind farms with STATCOM," in *2009 IEEE/PES Power Systems Conference and Exposition*, 2009, pp. 1-8: IEEE.

[15] A. Bozicek, B. Blazic, and I. Papic, "Mathematical modeling and current control of a voltage source converter," in *2008 43rd International Universities Power Engineering Conference*, 2008, pp. 1-5: IEEE.

[16] A. P. Jayam, "Application of STATCOM for improved dynamic performance of wind farms in a power grid," 2008.

[17] A. N. Zubidi, B. Ismail, I. M. A. Al Hamrounni, N. H. A. Rahman, and M. H. H. Mohd Rozlan, "The Impact of Integrating Multi-Microgrid System with FACTS Devices for Voltage Profile Enhancement and Real Power Loss Reduction in Power System: A Review," *Pertanika Journal of Science & Technology*, vol. 31, no. 2, 2023.

[18] Y. I. P. Darshini, K. Deepak, U. Chaithanya, Y. Hazarathaiah, D. Vannurappa, and S. G. Malla, "Power Quality Improvement of Standalone Microgrid during Faults on Distribution Line with DSTATCOM," in *2023 5th International Conference on Smart Systems and Inventive Technology (ICSSIT)*, 2023, pp. 530-536: IEEE.

[19] A. Mousaei, M. Gheisarnejad, and M. H. Khooban, "Challenges and Opportunities of FACTS Devices Interacting with Electric Vehicles in Distribution Networks: A Technological Review," 2023.

[20] P. V. S. S. A. Parimala, D. Sharma, and R. Mathew, "A comprehensive review on the advances in renewable wind power technology," *Wind Engineering*, vol. 47, no. 2, pp. 442-463, 2023.

[21] A. Noubrik, L. Chrifi-Alaoui, P. Bussy, and A. Benchaib, "Analysis and simulation of a crowbar protection for DFIG wind application during power systems disturbances," *Journal of Mechanics Engineering and Automation*, vol. 1, no. 4, pp. 303-312, 2012.

[22] S. Muller, M. Deicke, and R. W. De Doncker, "Doubly fed induction generator systems for wind turbines," *IEEE Industry applications magazine*, vol. 8, no. 3, pp. 26-33, 2002.

[23] M. C. Williams, "Fuel Cell Handbook, EG&G Technical Services," *Inc. Science Applications Int. Corp*, 2002.

[24] D. G. Photovoltaics and E. Storage, "IEEE standard for interconnection and interoperability of distributed energy resources with associated electric power systems interfaces," *IEEE Std*, vol. 1547, pp. 1547-2018, 2018.

[25] R. Allan, N. Jenkins, and F. Castro, "Large wind turbines and weak rural electricity systems," 1995.